Phys. Status Solidi A **206**, No. 2, 263–269 (2009) / **DOI** 10.1002/pssa.200824365

physica status solidi a
www.pss-a.com
applications and materials science

Structural characteristics of a multilayer of silicon rich oxide (SRO) with high Si content prepared by LPCVD

E. Quiroga[*,1], W. Bensch[1], Z. Yu[2], M. Aceves[2], R. A. De Souza[3], M. Martin[3], V. Zaporojtchenko[4], and F. Faupel[4]

[1] Institut für Anorganische Chemie der Universität Kiel, Max Eyth Str. 2, 24116 Kiel, Germany
[2] National Institute for Astrophysics, Optics and Electronics (INAOE), Calle Luis Enrique Erro 1, 72840 Tonantzitla, Pue., Mexico
[3] Institut für Physikalische Chemie, RWTH Aachen University, Landoltweg 2, 52056 Aachen, Germany
[4] Institut für Materialwissenschaft, Technische Fakultät der Universität Kiel, Kaiserstr. 2, 24143 Kiel, Germany

Received 4 September 2008, revised 25 November 2008, accepted 8 December 2008
Published online 22 January 2009

PACS 62.23.Pq, 68.37.–d, 68.65.Ac, 78.30.Hv, 79.60.Bm, 81.15.Gh

* Corresponding author: e-mail pesitrama@gmail.com, Phone: +49 431 880 2094

Single layer films and a multilayer structure of SRO (Silicon Rich Oxide) have been prepared by LPCVD (Low Pressure Chemical Vapour Deposition) and characterized by FTIR, SIMS, XPS, TEM and AFM measurements. The stacked structure is composed of alternating layers of SRO with high Si content and SRO with low Si content. The layered structure is confirmed by SIMS and TEM measurements. The composition of the materials is discussed. Besides Si nanocrystals, the existence of agglomerates of silicon oxide with structure close to fused silica and the existence of oxynitrides is evidenced in the films with high Si content.

1 Introduction SRO (Silicon Rich Oxide), also known as off-stoichiometric silicon oxide, is a material composed of Si agglomerates embedded in an oxide matrix. An indication of the Si content in the material is the parameter Ro, which is the ratio of the partial pressure of the precursor gases (for example, N_2O and SiH_4). SRO is an extensively studied material due to its interesting optoelectronic properties, such as photoluminescence in the visible range [1], which is ascribed to quantum confinement effects in the agglomerates of Si (commonly nanocrystals, nc) or to defects at their interfaces. Superlattices (SLs) and multilayer structures (MLs) could exhibit interesting quantum confinement effects too, due to the reduced size of their composing films. There are many reports about nc-Si/SiO_2 SLs and MLs that have mostly been prepared by PECVD (Plasma Enhanced Chemical Vapour Deposition) and magnetron sputtering [2–6]. Also epitaxial growth has been used [7]; however, there are just a few reports of MLs prepared by LPCVD [8]. Most of the works present MOS-like structures with embedded nanocrystals [9, 10]. On the other hand, to our knowledge there are no reported multilayer structures based on SRO with a high Si content prepared by LPCVD. LPCVD is a very simple method for film deposition and is thoroughly compatible with Si technology. Furthermore, it permits an easy variation of the silicon content of the deposited layers in a wide range.

In this work, a multilayer structure composed of two different layers of SRO, one with high silicon excess, deposited by LPCVD are studied. FTIR (Fourier Transform Infrared), XPS (X-ray Photoelectron Spectroscopy), SIMS (Secondary Ion Mass Spectroscopy), TEM (Transmission Electron Microscopy) and AFM (Atomic Force Microscopy) measurements were performed in order to study the composition and structural characteristics of the multilayer. In addition, single layers of SRO with the same characteristics as that of the multilayer were studied for comparison.

2 Experimental SRO single layers with Ro = 1 (SRO1) and Ro = 50 (SRO50), and a multilayer structure composed of the stacks of SRO1 and SRO50 were deposited on p-type Si(100) wafers with 30–50 Ω cm resistivity

Table 1 Deposited samples.

sample	layer	thickness (nm)
SRO1	single layer	133
SRO50	single layer	60.8
multilayer	first* layer of SRO50	11
	first layer of SRO1	23
	second layer of SRO50	~21
	second layer of SRO1	~21
	third layer of SRO50	~23

* The layers are numbered parting from the substrate.

by LPCVD at 725 °C, using SiH_4 and N_2O as the precursor gases. A list of the deposited samples is shown in Table 1. The multilayer is composed of 2 periods of films: 3 barrier layers of SRO50 and 2 well layers of SRO1. The deposition of the multilayer was done varying manually the precursor gases during the deposition.

The microstructure of the samples was studied with TEM measurements (Tecnai F30, 300 kV). Measurements of the roughness of the films were performed with an AFM Autoprobe CP (Park Scientific Instruments) in contact mode, which has a lateral resolution of 0.025 nm and a vertical resolution of 0.0025 nm.

SIMS measurements were performed on a Time-of-Flight SIMS machine (TOF-SIMS IV, IONTOF, Münster). Secondary ions for analysis were produced by bombardment with 15 keV Ga^+ ions. Sputter etching of the sample surface was accomplished by bombardment with 1 keV Cs^+ ions for negative secondary ion analysis, and with 2 keV Cs^+ ions for positive secondary ion analysis (the higher yield of MCs^+ secondary ions at 2 keV was more important than the reduced depth resolution). XPS analysis was carried out with an electron spectrometer (Omicron) equipped with a non-monochromated Al Ka source at 0° take off angle. For these measurements, the samples were previously sputtered in a preparation chamber (Omicron Full Lab) bombarding the samples with argon ions with a kinetic energy of 1 keV at an incident angle of 36° for 5 min.

FTIR spectra of the films were measured with a Bruker FTIR spectrometer model V22, which works in the range of 4000–350 cm^{-1} with 2 cm^{-1} resolution.

3 Results and discussion

3.1 TEM and AFM measurements A typical TEM micrograph of SRO1 is shown in Fig. 1. Two phases could be easily distinguished: nanocrystalline Si and amorphous silicon oxide. The material presents good phase separation, and most of the SRO1 film is composed of zones of crystalline Si. Therefore, it can be considered as agglomerates of silicon oxide embedded in a crystalline silicon matrix.

The layered structure of the multilayer can be seen in Fig. 2. According to the TEM micrograph, the total thickness of the multilayer can be estimated to be about 100 nm. The different layers are clearly discernible.

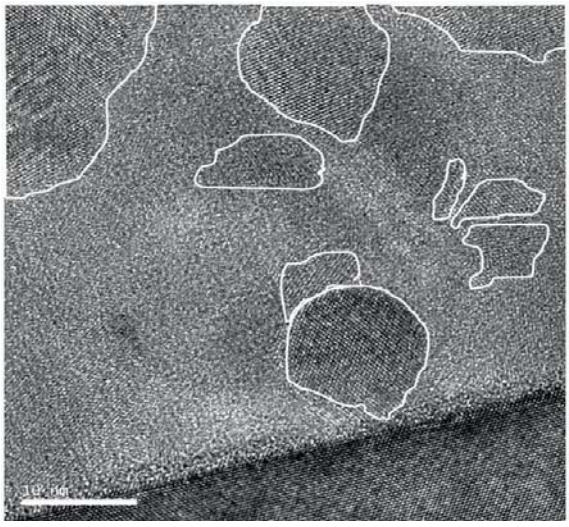

Figure 1 TEM micrograph of SRO Ro = 1. For an easier identification the areas containing Si nanocrystals are enclosed with white lines.

The first layer of SRO50 in the multilayer (from the substrate's side) is very uniform, with a thickness of ~10 nm. On the other hand, the bottom interface of the first layer of SRO1 is very well defined, but its top interface is very rough. This is an indication of the large difference in roughness between the SRO1 and SRO50 films. The large roughness of the SRO1 layer is due to the formation of Si nanocrystals during the deposition process. The layers deposited onto the first SRO1 layer are then relatively rough, but are still easily distinguishable. Figure 3 shows an AFM micrograph of the single SRO1 layer denoting the large roughness of this material.

The mean peak height of the surface bumps is 41 nm and represents ~30% of the total film thickness. The multilayer exhibits a rough surface too (image not shown) with the mean peak height of the surface bumps being 34 nm.

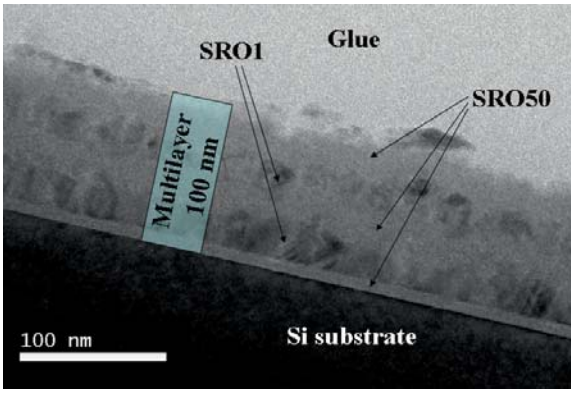

Figure 2 (online colour at: www.pss-a.com) TEM micrograph of the multilayer. The layers of SRO50 are the smooth zones, and the SRO1 layers look like protuberances (Si nanocrystals). The total thickness of the sample is ~100 nm.

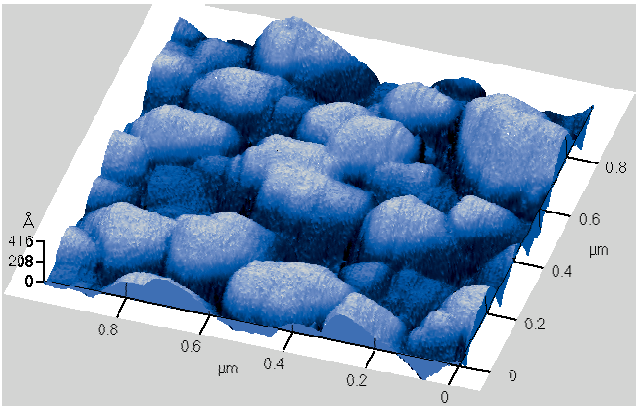

Figure 3 (online colour at: www.pss-a.com) Three dimensional AFM image of the surface of the film SRO Ro = 1. The mean peak height of the surface bumps corresponds to ~30% of the film thickness.

3.2 SIMS measurements Figure 4 shows a ToF-SIMS depth profile of the multilayer. The distribution of O, Si and N were detected from SiO_2^-, Si_2^- and SiN^- ions respectively. This does not mean that the sample contains these compounds but indicates the presence of the mentioned elements together in the sample. As expected, the Si_2^- and SiO_2^- signals show variations complementary to each other, again indicating that a layered structure was deposited. Interestingly, the multilayer also contains nitrogen. The SiN^- signal disappears at the interface multilayer/silicon substrate, as happens with the SiO_2^- signal, demonstrating that nitrogen and oxygen are only present in the multilayer. Nevertheless, the intensity of the SiN^- signal is only about 1% of the intensity of the Si_2^- signal.

The low intensity of the SiN^- signal could be an evidence of the small amount of N in SRO1, but without knowing the relative ionisation probabilities of SiO_2^-, Si_2^- and SiN^- it is not possible to determine its amount. The N atoms in the multilayer may enhance a possible photoluminescence effect (PL) from the Si nanocrystals in the as-deposited sample [11, 12]. Nevertheless the N content in the present samples is very low and may not have a significant effect on the PL intensity. Eventhough, only PL measurements and analyses will provide the answer to the question how N influences the PL properties. Such PL measurements will be performed in the near future.

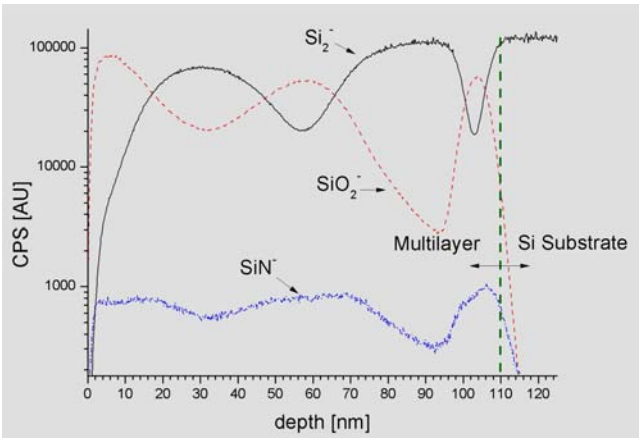

Figure 4 (online colour at: www.pss-a.com) ToF-SIMS depth profile of the multilayer. The elemental distributions of O, Si and N have been detected as Si_2^-, SiO_2^- and SiN^-.

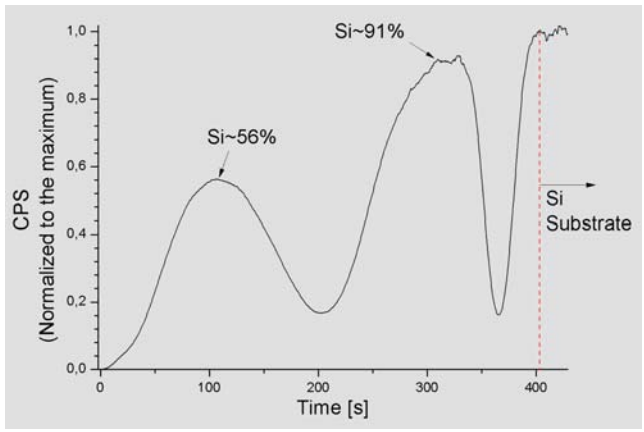

Figure 5 (online colour at: www.pss-a.com) Normalized ToF-SIMS Si_2^- signal as a function of sputter time. The silicon concentration apparently increases, from ~56% of the outer layer of SRO1 to ~91% of the next layer.

Figure 5 shows the normalized Si_2^- signal. From this figure it can be deduced that the Si content is reduced in the outer SRO1 layer. The intensity of the Si_2^- signal from the first SRO50 layer (to the substrate's side), is around 10% compared to that from the Si substrate. As a consequence it can be concluded that the probability to obtain Si_2^- ions from the SRO50 layer is around 10% compared with the probability to obtain such ions from the Si substrate. Since SRO1 presents a very good phase separation and Si nanocrystals represent its major phase (see TEM micrograph), the SIMS Si_2^- signal corresponds mainly to the Si nanocrystals and the matrix effects to obtain it should be less significant. In this way, an approximation of the concentration of Si was made taking into account the maxima of the Si_2^- signal. In the outer SRO1 layer it is about 56%, and it amounts to about 91% in the other layer of the same material. SIMS analysis of positive ions was also carried to confirm the Si profile, since it is far less sensitive to matrix effects. The obtained spectrum (Fig. 6) presents the same behaviour as the one obtained with negative ions, with close values (and much closer when the Si content in the sample is larger) but with a much poorer resolution. Nevertheless, even when the concordance of SIMS measurements of positive and negative ions indicate a good approximation of the Si concentration in SRO1 layers, the exact value can not be determined by this method alone.

The graded concentration of Si in the multilayer may be caused by residual gases in the LPCVD chamber due to the manual variation of the gas flow, which give the opportunity to obtain more silicon oxide. This experimental fac-

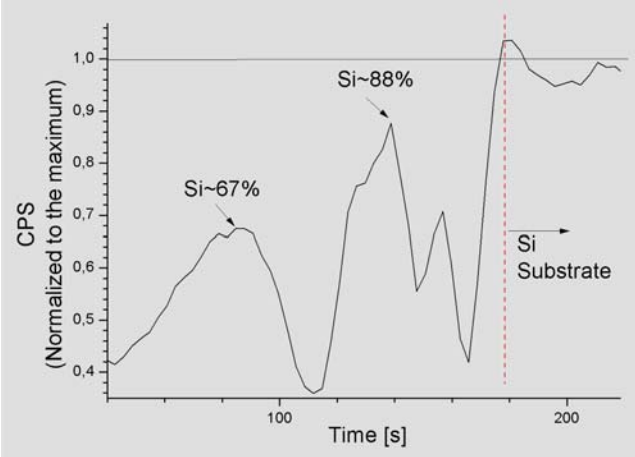

Figure 6 (online colour at: www.pss-a.com) Positive SIMS normalized spectra of the $SiCs^+$ signal (Si is detected in the way of $SiCs^+$ ions). The silicon concentration increase in depth, as was also evidenced with the SIMS of negative ions.

tor must be taken into account if many layers should be deposited.

3.3 XPS measurements In the study of Si oxides by XPS, the oxidation states of Si can be estimated from the chemical shifts of the Si 2p core level line [13, 14]. The Si 2p spectrum of silicon oxides contains contributions of the spin orbit Si $2p_{1/2}$ and Si $2p_{3/2}$ lines [13, 15–17] being separated by 0.6 eV. This is an atomic property, practically independent of the chemical environment [15].

In the XPS spectra, each Si 2p core level line occurs at positions corresponding to the energy shifts from the different oxidation states of Si (Si^0, Si^{1+}, Si^{2+}, Si^{3+}, Si^{4+}). The position of the peaks corresponding to Si^0 and Si^{4+} (SiO_2) is well known and is easily distinguishable [16]. On the other hand, the peaks related with silicon sub-oxides have been

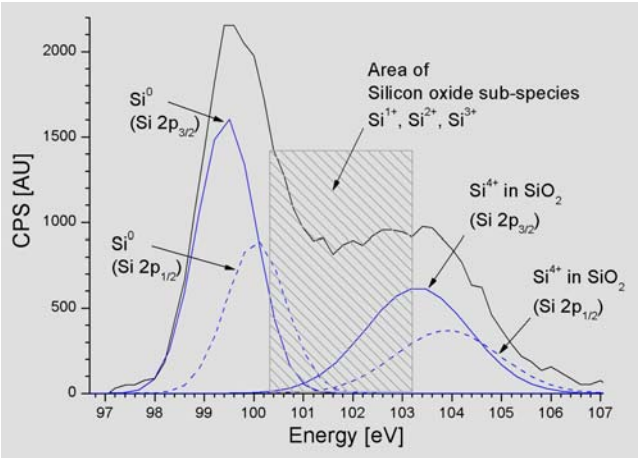

Figure 7 (online colour at: www.pss-a.com) XPS spectrum of SRO1. The peaks of the Si $2p_{1/2}$ and Si $2p_{3/2}$ of Si^0 and Si^{4+} were fitted. The existence of sub-oxide species can be noted in the region between Si^0 and Si^{4+}.

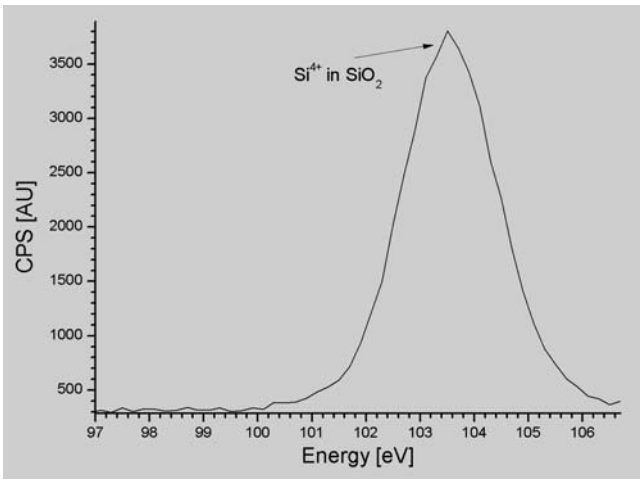

Figure 8 XPS spectrum of SRO50. Just the contribution of SiO_2 could be observed in the spectrum.

studied at Si/SiO_2 interfaces [13, 14, 17, 18], but they cannot be distinguished unequivocally in a complex spectrum composed of different Si oxide species. Hence, a quantitative analysis of such highly convoluted spectra is not straightforward and the results obtained by such fittings sensitively depend on the fitting parameters applied.

In the XPS spectra, each Si 2p core level line occurs at positions corresponding to the energy shifts from the different oxidation states of Si (Si^0, Si^{1+}, Si^{2+}, Si^{3+}, Si^{4+}). The position of the peaks corresponding to Si^0 and Si^{4+} (SiO_2) is well known and is easily distinguishable [16]. On the other hand, the peaks related with silicon sub-oxides have been studied at Si/SiO_2 interfaces [13, 14, 17, 18], but they cannot be distinguished unequivocally in a complex spectrum composed of different Si oxide species. Hence, a quantitative analysis of such highly convoluted spectra is not straightforward and the results obtained by such fittings sensitively depend on the fitting parameters applied.

The XPS Si 2p spectrum of the surface of SRO1 is shown in Fig. 7. For elemental Si the signal of the Si $2p_{3/2}$ line is found at 99.45 eV and that of Si $2p_{1/2}$ at 100.05 eV, both having a FWHM of 1.2 eV. For Si^{4+} the corresponding signals occur at at 103.3 eV and at 103.9 eV with a FWHM of 2.1 eV for both emissions. The peaks of the Si sub-oxides are located in the region between these two species. As an individual assignment of SiO_x sub-oxides is not unambiguously possible, all the sub-oxides are considered as one group. The amount of sub-oxides was obtained by subtracting the area of the fitted peaks of Si^0 and Si^{4+} from the total area. According to the fitting procedures, the top region of the SRO1 film consists of 50% of elemental Si (Si^0), 34% of SiO_2 (Si^{4+}) and 16% of SiO_x (Si^{1-3+}) with $0 < x < 2$. The value of the amount of Si on the surface of SRO1 is very close to the amount of Si in the outer layer of SRO1 in the multilayer. This result is expected, since the concentration of Si is reduced going from the substrate to the top of the samples with deposition time, and the deposition time to obtain SRO1 and the multilayer are similar.

The high amount of silicon sub-oxides in SRO1 is the result of the large amount of Si/SiO_2 interfaces that exist in this material. In contrast, in the XPS spectrum of the single SRO50 layer just the contribution of SiO_2 could be observed (Fig. 8) evidencing that this material is practically SiO_2. Only possible differences in density and the degree of disorder in the Si–O environments within the material compared with a thermal stoichiometric oxide can be expected.

3.4 FTIR spectra Figure 9 shows the FTIR spectra of the samples SRO1, SRO50 and of the multilayer in the range of 900 cm^{-1} to 1300 cm^{-1}. The absorption curves were normalized for clarity. The real peak intensity of sample SRO1 is around 3 times lower than that of the other samples. As can be noted in sample SRO50 just the typical absorptions of SiO_2 are evident (peaks B and D).

Peak B located at 1064 cm^{-1} corresponds to the Si–O TO (Transverse Optic) stretching vibration [19–22], and peak D occurring, as a shoulder at 1140 cm^{-1}, corresponds to the Si–O TO asymmetric stretching mode [21, 23]. The position of these bands corresponds to as-deposited Silicon Rich Oxide with low silicon excess [24]. The number of considered bands is consistent with the deconvolution of the peak centred at 1064 cm^{-1} in two peaks, as proposed by some authors studying thin thermal SiO_2 films [25, 26].

On the other hand, in the sample SRO1 the absorption peaks A, C and E are evident. Peak A, at 966 cm^{-1}, has been found by some groups as an indication of the existence of nitrogen in Si ingots. The intensity of this peak increases with increasing exposure time of the ingots to N_2 atmosphere [27]. Silicon nitride films prepared by nitridation of silica also exhibit this peak [28], and it is explained

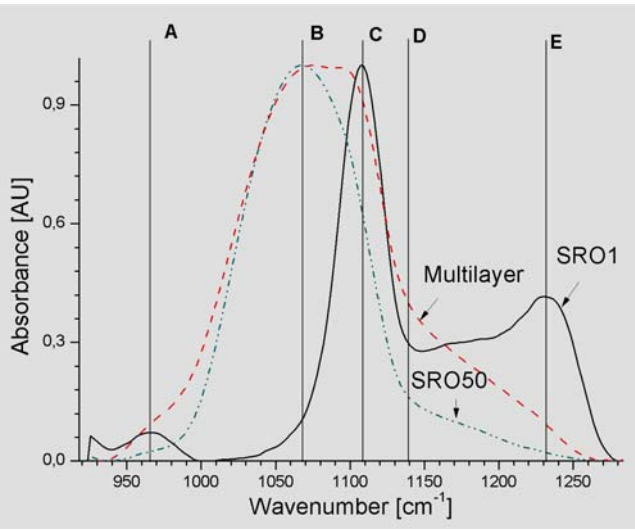

Figure 9 (online colour at: www.pss-a.com) Absorption spectra of the different samples. Five absorption peaks could be identified: A (966 cm^{-1}) related with some N in the films, and peaks B (1064 cm^{-1}), C (1107 cm^{-1}), D (1140 cm^{-1}) and E (1233 cm^{-1}) that are related with Si–O bonds.

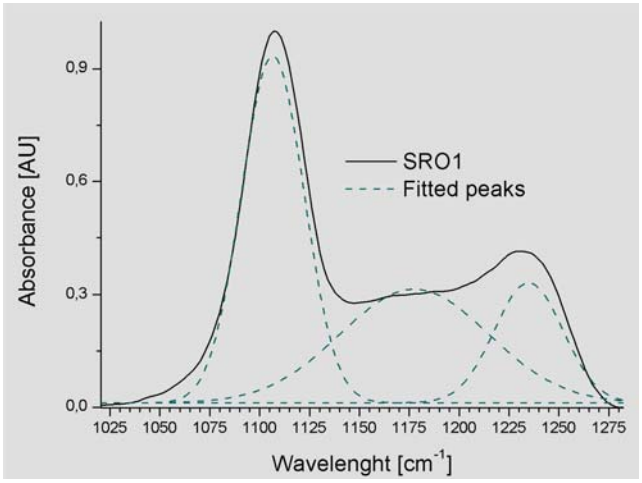

Figure 10 (online colour at: www.pss-a.com) Deconvolution of the absorption spectrum of the film of SRO Ro = 1. Besides the peaks C (1107 cm^{-1}) and E (1233 cm^{-1}) an absorption peak at 1178 cm^{-1} can be observed, which is related to TO Si–O asymmetric stretching vibration.

as the Si–N–Si asymmetric stretching vibration in SiN_4 tetrahedra joined via corners with SiO_4 tetrahedra. Nevertheless, this vibration has not only been observed on crystalline Si or crystalline silicon oxide, but also on polysilicon films annealed in N_2 and is accompanied by oxygen incorporation in the films [29]. As the SRO Ro = 1 is a material close to SIPOS (Semi-Insulating Polysilicon, see TEM results), the idea of oxynitrides in these films is very feasible. Because peak A only appears for SRO1 and not in SRO50, it can be concluded that both materials contain N (as evidenced by SIMS), but only in SRO1 N is bonded to Si in tetrahedral configuration along with oxygen forming a type of oxynitride. The N in SRO50 may be located on interstitial positions, presenting a different bonding configuration since the FTIR spectrum of this material does not show any characteristic peaks of silicon nitrides or oxynitrides.

Peak C being centred at 1107 cm^{-1} in SRO1 occurs on a position which has been reported as interstitial oxygen in Si ingots [30, 31] and at Si/SiO_2 interfaces [21]. It has been reported that the TO Si–O stretching vibration of segregated oxygen in polysilicon also produces this absorption peak [29], and actually coincides with the Si–O TO stretching vibration in fused silica [31, 32]. It has been proposed that the interstitial oxygen in Si could adopt a structure close to that of fused silica, but with the Si–O–Si bond angle of around 100°, ascribing then the absorption peak at 1107 cm^{-1} to the TO Si–O stretching vibration [31]. As the SRO Ro = 1 is a material close to SIPOS this absorption peak could be expected.

The deconvoluted IR spectrum of SRO1 (Fig. 10) shows an extra absorption at 1178 cm^{-1} which is blue-shifted by 38 cm^{-1} with respect to the Si–O TO asymmetric stretching vibration of SRO50. This value is very close to the blue-shift of peak C with respect to the TO Si–O

stretching vibration of SRO50 (43 cm^{-1}). According to this analysis, peak C and the one located at 1178 cm^{-1} may be caused by TO Si–O stretching vibrations of silicon oxide agglomerates with bonding angles and Si–O bond lengths close to those of quartz. In fact, according to the TEM micrograph of SRO1 in Fig. 1, this material can be considered as agglomerates of silicon oxide embedded in a nanocrystalline silicon matrix. The consideration of two peaks for the Si–O TO vibrations of SRO1 agrees with the number of vibrations found in SiO_2 films with thickness lower than 40 nm [26].

Peak E (at 1233 cm^{-1}) is related to LO Si–O vibrations [26, 33]. LO vibrations are inactive in normal incidence of the IR light, but it has been found that they become active when the particles of silicon oxide have a platelet shape with size <0.36 μm [21, 29, 30]. The agglomerates of silicon oxide in SRO1 are much smaller than this size in all their dimensions, as can be observed in Fig. 1.

The IR spectrum of the multilayer shows all 5 absorption peaks (with peaks A, D and E as shoulders), as can be seen in Fig. 9. Peaks B and C can be identified as the extremes of an asymmetric peak centred at ~1090 cm^{-1}.

The positions of all peaks in the multilayer remain very close to the ones in SRO Ro = 1 and Ro = 50. This evidences that 2 phases coexist in the multilayer, in accordance with the results of TEM and SIMS investigations. The distinction of the two phases is a good indicator that the composing materials do not react with the subsequent layers during the deposition procedure.

4 Conclusion The creation of a multilayer structure of SRO with high Si content by LPCVD has been evidenced by TEM and SIMS measurements. The multilayer is composed of layers of SRO1 and SRO50. A couple of technological constraints have been found to obtain a multilayer by LPCVD: SRO1 presents a high roughness and the amount of silicon in this material diminishes along the layer thickness. A layered structure of two independent phases was obtained even with the existing constraints. All results demonstrate that it is possible to produce layered structures by LPCVD, but the fact that silicon diminishes has to be taken into account.

Si-nanocrystals are the major component of SRO1, and agglomerates of silicon oxide with reduced size are the minor phase. The agglomerates of silicon oxide may have a structure close to fused silica, as evidenced by FTIR. The large amount of silicon sub-oxides found in SRO1 may be due to the large amount of Si/SiO_2 interfaces in this material.

Nitrogen is present in small amounts in the whole multilayer, but it is present as oxynitrides only in the layers of SRO1. Nevertheless the contribution of the oxynitrides to the total composition of SRO1 should be in a very low range. In SRO50 the nitrogen is thought as interstitial.

Acknowledgements The authors appreciate the support from CONACyT and DAAD.

References

[1] D. Berman, M. Aceves, A. Gallegos, A. Morales, L. R. Berriel, J. Carrillo, F. Flores, C. Falcony, C. Domínguez, A. Llobera, M. Riera, and J. Pedraza, Phys. Status Solidi C **1**(S1), S83–S87 (2004).
[2] L. Tsybeskov, Technical Proc. of the 2002 Int. Conf. on Computational Nanoscience and Nanotechnology, Molecular and Nanotechnology (2002), chap. 12, p. 304.
[3] L. Tsybeskov, K. D. Hirschman, S. P. Duttagupta, M. Zacharias, and P. M. Fauchet, Appl. Phys. Lett. **72**(1), 43 (1998).
[4] V. Duzhko and L. Tsybeskov, Appl. Phys. Lett. **83**(25), 5229 (2000).
[5] M. Zacharias, J. Bläsing, and P. Veit, Appl. Phys. Lett. **74**(18), 2614 (1999).
[6] L. Tsybeskov, G. F. Grom, and P. M. Fauchet, Appl. Phys. Lett. **75**(15), 2265 (1999).
[7] G. F. Grom, D. J. Lockwood, J. P. McCaffrey, H. J. Labbé, P. M. Fauchet, B. White, Jr., J. Dlener, D. Kovalev, F. Koch, and L. Tsybeskov, Nature **407**, 358 (2000).
[8] M. Modreanu, E. Aperathitis, M. Androulidaki, M. Audier, and O. Chaix-Pluchery, Opt. Mater. **27**, 1020 (2005).
[9] D. N. Kouvastos, V. Ioanou-Sougleridis, and A. G. Nassiopoulou, Appl. Phys. Lett. **8**(3), 397 (2003).
[10] V. Ioanou-Sougleridis and A. G. Nassiopoulou, J. Appl. Phys. **94**(6), 4084 (2003).
[11] R. López-Estopier, M. Aceves-Mijares, and C. Falcony, in: Proceedings 2006 3rd Int. Conf. on Electrical and Electronics Engineering (ICEEE), Mexico City, Mexico, 2006 (IEEE, 2006).
[12] R. López-Estopier, M. Aceves-Mijares, J. Carrillo, Z. Yu, and C. Falcony, in: Proceedings 2nd Int. Conf. on Electrical and Electronics Engineering (ICEEE) and XI Conference on Electrical Engineering (CIE 2005), Mexico City, Mexico, 2005 (IEEE, 2005), pp. 227–230.
[13] G. Hollinger and F. J. Himpsel, Appl. Phys. Lett. **44**, 93 (1984).
[14] F. J. Grundthaner, P. J. Grundthaner, R. P. Vasquez, B. F. Lewis, and J. Maserjian, Phys. Rev. Lett. **43**(22), 1683 (1979).
[15] F. J. Himpsel, F. R. McFeely, A. Taleb-Ibrahimi, J. A. Yarmoff, and G. Hollinger, Phys. Rev. B **38**(9), 6084 (1988).
[16] F. Verpoort, P. Persoon, L. Fiermans, G. Dedoncker, and L. Verdonck, J. Chem. Soc., Faraday Trans. **93**, 3555 (1997).
[17] P. J. Grundthaner, M. H. Hecht, F. J. Grundthaner, and N. M. Johnson, J. Appl. Phys. **61**(2), 629 (1987).
[18] K. Hirose, H. Nohira, K. Azuma, and T. Hattori, Prog. Surf. Sci. **82**, 3 (2007).
[19] J. Serra, E. G. Parada, P. González, D. Fernández, S. Chiussi, J. Pou, B. León, and M. Pérez-Amor, Surf. Coat. Technol. **80**, 211 (1996).
[20] P. Mandracci and C. Ricciardi, Thin Solid Films **515**, 7639 (2007).
[21] J. Niu, D. Yang, J. Sha, J. N. Wang, and M. Li, Mater. Lett. **61**, 894 (2007).
[22] A. Lehmann, L. Schumann, and K. Hübner, Phys. Status Solidi B **121**, 505 (1984).
[23] F. Ay and A. Aydinly, Opt. Mater. **26**, 33 (2004).
[24] A. Morales, J. Barreto, C. Domínguez, M. Riera, M. Aceves, and J. Carrillo, Physica E **38**, 54 (2007).

[25] I. W. Boyd, Appl. Phys. Lett. **51**(6), 418 (1987).
[26] I. P. Lisovskii, V. G. Litovchenko, V. G. Lozinskii, and G. I. Steblovskii, Thin Solid Films **213**, 164 (1992).
[27] J. Itoh, T. Nozaki, and T. Masui, T. Abe, Appl. Phys. Lett. **47**(3), 488 (1985).
[28] P. S. Lakshminarasimham and P. S. Gopalakrishnan, J. Mater. Sci. Lett. **14**, 1801 (1995).
[29] D. Gupta, B. Awasthy, and S. P. Varma, J. Mater. Sci. **28**, 1488 (1993).
[30] A. Borghesi, M. Geddo, and B. Pivac, J. Appl. Phys. **69**(10), 7251 (1991).
[31] W. Kaiser, P. H. Keck, and C. F. Lange, Phys. Rev. **101**(4), 1264 (1956).
[32] G. Gu, P. P. Ong, and C. Chu, J. Phys. Chem. Solids **60**, 943 (1999).
[33] W. Bensch and W. Bergholz, Semicond. Sci. Technol. **5**, 421–428 (1990).